pharmaceutics

MDPI

Article

Innovative Oral GLP1 Receptor Agonist Dosage Forms: Additive Manufacturing Solutions Enhance Bioavailability

Emily Aedtner [1], Paula Nitschke [1], Marcel Enke [1], Moritz Bünger [2], Pia Heintze [3], Hauke Lilie [4], Klaus Kühne [1,5], Andrea Buzanich-Ladinig [2], Anne Seidlitz [3] and Achim Schneeberger [1,5,*]

1 Laxxon Medical GmbH, Otto-Schott Str. 15, 07745 Jena, Germany; emily.aedtner@laxxonmedical.com (E.A.); paula.nitschke@laxxonmedical.com (P.N.); marcel.enke@laxxonmedical.com (M.E.); klaus.kuehne@laxxonmedical.com (K.K.)
2 Clinical Centre for Population Medicine in Fish, Pigs and Poultry, University of Veterinary Medicine, Veterinaerplatz 1, 1210 Vienna, Austria; moritz.buenger@vetmeduni.ac.at (M.B.); andrea.ladinig@vetmeduni.ac.at (A.B.-L.)
3 Pharmaceutical Technology, Institute of Pharmacy, Freie Universität Berlin, Kelchstraße 31, 12169 Berlin, Germany; p.heintze@fu-berlin.de (P.H.); anne.seidlitz@fu-berlin.de (A.S.)
4 Institute for Biochemistry and Biotechnology/Technical Biochemistry, Martin-Luther-Universität Halle-Wittenberg, Kurt-Mothes-Straße 3, 06120 Halle, Germany; hauke.lilie@biochemtech.uni-halle.de
5 Laxxon Medical Corp, 261 Madison Ave, New York, NY 10016, USA
* Correspondence: achim.schneeberger@laxxonmedical.com

Abstract

Introduction: Current methods of orally delivering peptide therapeutics have low bioavailability. There is an increasing medical need for oral peptide therapeutics. Three-dimensional (3D) screen printing (3DSP), based on its high flexibility in terms of tablet size, architecture and excipients, could enable dosage forms yielding increased oral bioavailability of peptides, including liraglutide (LG) and semaglutide (SG), in a mass-production context. **Methods**: 3DSP technology was used to manufacture oral dosage forms containing the peptides LG or semaglutide along with permeation enhancers, alone or in combination. LG was used as a model peptide to evaluate the effect of tablet size and permeation enhancers. Conventional-size oblong tablets and microtablets were compared. Microtablets were produced using stencil printing, a variation of 3DSP, and then placed in enteric capsules to tailor drug release to the small intestine. As a next step, SG was used in an advanced microtablet formulation. This allowed benchmarking to marketed oral SG (Rybelsus®). The resulting dosage forms were characterized by applying appropriate in vitro methods and PK studies. **Results**: 3D screen and stencil printing allowed manufacturing of conventional-size tablets and microtablets with high loads of permeation enhancers, respectively. In vitro testing showed acceptable uniformity for both formats. Dissolution studies revealed peptide release to be controlled by the tablet size, the formulation and the enteric capsules. PK studies demonstrated the importance of permeation enhancers for oral peptide bioavailability. The microtablet/enteric capsule concept tested revealed promising in vivo results for both LG and SG. **Conclusions**: This study was designed to explore the potential of 3D screen-/stencil-printing technology to improve the bioavailability of orally administered peptides. The proposed approach, involving microtablets formulated for intestinal delivery using enteric capsules, showed promising results in enhancing the oral bioavailability of LG and SG, with SG achieving exposition levels comparable to those reported for the marketed reference product.

Keywords: 3D printing; additive manufacturing; oral peptides; GLP-1 receptor agonist; liraglutide; semaglutide; permeation enhancer; oral bioavailability

Check for updates

Academic Editor: Peter Timmins

Received: 17 October 2026
Revised: 17 November 2026
Accepted: 24 November 2026
Published: 27 November 2026

Copyright: © 2026 by the authors. Licensee MDPI, Basel, Switzerland. This article is an open access article distributed under the terms and conditions of the Creative Commons Attribution (CC BY) license.

1. Introduction

Glucagon-like peptide-1 (GLP-1) is an endogenous incretin hormone that plays a central role in glucose homeostasis by stimulating glucose-dependent insulin secretion, suppressing glucagon release, delaying gastric emptying, and reducing postprandial glucose excursions. Beyond its metabolic actions, GLP-1 receptor activation in the central nervous system decreases appetite and food intake, resulting in sustained weight loss. Consequently, GLP-1 receptor agonists (GLP-1-RAs) have become established therapies for both type 2 diabetes mellitus and obesity and additionally provide cardiovascular benefits, including reductions in major adverse cardiovascular events [1–3]. Beyond their established metabolic indications, GLP-1-RAs are increasingly recognized as a versatile therapeutic class with potential benefits for nervous system disorders, including stroke and inflammatory conditions, further expanding their potential clinical relevance [4–7].

Native GLP-1 has a plasma half-life of only approximately two minutes because of rapid degradation by dipeptidyl peptidase IV (DPP-IV) and neprilysin, limiting its therapeutic utility [8–11]. To overcome this limitation, long-acting GLP-1-RAs such as LG and SG were developed through structural modifications that improve resistance to enzymatic degradation and prolong systemic exposure. LG, a C16 fatty acid-conjugated GLP-1-RA, provides 24 h exposure following once-daily subcutaneous (s.c.) administration, whereas SG incorporates additional amino acid substitutions and a C18 fatty diacid conjugate, extending its half-life to approximately one week and enabling once-weekly dosing [12–14]. Current clinical guidelines recommend GLP-1-RAs for patients with type 2 diabetes mellitus, particularly those with established cardiovascular disease or a high risk of cardiovascular disease, due to their favorable efficacy and safety profiles [15].

Achieving oral delivery of peptide therapeutics is an important goal in drug development, as it could overcome the limitations of injectable administration, improve patient convenience and acceptance, and enhance treatment adherence, particularly in chronic diseases requiring long-term therapy. Reported reasons for discontinuing injectable diabetes medications include inconvenience (35.7%), preference for oral medication (34.2%), pain (25.4%), concerns about needle size (23.4%), and injection-site reactions (s.c. SG (6.6%) vs. placebo (9.9%)) [16,17]. Oral dosage forms may also reduce the burden on healthcare systems by enabling self-administration and simplifying drug distribution. Given the growing clinical importance of oral peptide therapeutics (examples include marketed products such as SG (Rybelsus®/Wegovy®) for diabetes, Octreotide (Mycapssa®) for acromegaly (approved), Icotrokinra for psoriasis, and Enlicitide for hypercholesterinemia), investigating innovative oral delivery technologies is essential to overcome barriers such as enzymatic degradation, poor intestinal permeability, and variable bioavailability, ultimately expanding the therapeutic potential and accessibility of this drug class [18–23].

Despite recent advances in oral peptide delivery, systemic bioavailability remains generally low, typically below 1–2% for currently established formulations [24,25]. Oral SG, formulated with the absorption enhancer SNAC, achieves an absolute bioavailability of approximately 0.4–2%, while oral octreotide formulations exhibit a bioavailability of around 0.5–1% [26,27]. These low absorption rates reflect substantial gastrointestinal enzymatic degradation and limited epithelial permeability, often resulting in high dose requirements and considerable inter- and intraindividual variability. Consequently, improving oral bioavailability, absorption consistency and formulation efficiency remains a major objective in peptide drug development.

Permeation enhancers have emerged as key elements for oral peptide delivery. The permeation enhancer N-(8-[2-hydroxybenzoyl] amino) caprylate (SNAC) is used in the marketed oral SG dosage forms Rybelsus® and Wegovy®. SNAC transiently increases transcellular gastric absorption while locally buffering the microenvironment to reduce peptide

degradation, thereby enabling clinically relevant oral bioavailability [24,25]. Technologies such as GIPET™ utilize medium-chain fatty acid-based enhancers, including C10, to transiently and reversibly increase epithelial permeability, improving the absorption of peptides and other macromolecules [28–31]. Among the best-characterized enhancers, sodium caprate (C10, realized in the Enlicitide formulation) promotes reversible opening of intestinal tight junctions and has enabled oral delivery of peptides and antisense oligonucleotides, while SNAC primarily enhances transcellular gastric uptake through localized effects on epithelial permeability and the luminal microenvironment [22,24,25,28–30,32–35]. Despite these advances, manufacturing conventional tablets containing the high concentrations of permeation enhancers required for effective absorption remains challenging. At high enhancer loadings, tabletability, compactibility, and compressibility are compromised, making robust formulation development by direct compression difficult [36]. Recently, Xu et al. proposed an interesting approach to overcoming these problems. They used 3D fused deposition modeling to manufacture a capsule containing peptide and C10 powder in separate compartments, designed to release both components constantly. They have so far provided in vitro proof of principle, which awaits in vivo testing [37]. Bluemlinger et al. conducted a systematic investigation into the importance of peptide release within the gastrointestinal tract. To this end, they used capsules with different enteric coatings. They found that targeting peptide release to the ileum maximized the absorption of semaglutide [38].

3DSP has emerged as an innovative pharmaceutical manufacturing technology capable of producing complex dosage forms with formulation flexibility, high precision and scalability [39]. 3DSP, as demonstrated by SPID®, is an additive manufacturing technique, which involves spreading of a semisolid base (printing paste) containing the drug, excipients and a solvent/dispersing agent onto a screen and then pushing it through the openings via a blade or squeegee. After a short drying period, paste for the subsequent layer is pushed through the screen and deposited on top of the previous layer, building the object layer by layer. One variation of screen printing uses a stencil instead of a screen. This furthers the technology's flexibility in relation to excipients and allows for shorter printing times. In contrast to conventional tableting, 3DSP and its variations enable the fabrication of multicompartment dosage forms with defined geometry and tailored release characteristics while accommodating formulations containing high concentrations of permeation enhancers. Furthermore, 3DSP allows for the production of small tablets. It is possible to produce tablets with a diameter below 1 mm. Such microtablets possess a substantially higher surface area-to-volume ratio than conventional-size tablets, promoting rapid disintegration and dissolution and generating high local concentrations of both drug and permeation enhancer at the absorption site [40–43].

In the present study, we investigated whether combining C10 and the related fatty acid permeation enhancer sodium caprylate (C8) in 3D screen-printed microtablets could enhance the oral bioavailability of peptides such as LG and SG. In addition, microtablets were packed into enteric capsules. This microtablet/enteric capsule approach was designed with the idea of site-specific release in the small intestine following capsule disintegration, thereby minimizing premature peptide exposure during gastrointestinal transit while maximizing the simultaneous local release of peptides and permeation enhancers [38]. This formulation strategy markedly improved the oral bioavailability of LG compared with the conventional tablet size/form based on C10. The strategy was then successfully translated to SG, with Labrasol® ALF serving as a solubilizer. Labrosal® was found to be readily compatible with the aqueous pastes used in SPID®. It is expected to be in close association with the peptide, SG, within the paste and the resulting tablet, thereby supporting peptide absorption upon release. Together, these studies demonstrate the potential of SPID® as a versatile platform for oral delivery of peptides, including GLP-1-RAs such as LG and SG.

2. Materials and Methods

2.1. Chemicals

LG and SG were purchased from Bachem, Bubendorf, Switzerland. The various excipients were purchased from established providers: hydroxypropyl cellulose (HPC) (Klucel LF; Ashland, Covington, KY, USA), hydroxypropyl methylcellulose (HPMC) (Benecel K4M; Ashland, Covington, KY, USA), low-substituted HPC (L-HPC LH-31; Shin Etsu, Tokyo, Japan), microcrystalline cellulose (MCC) (Avicel PH 105; Dupont, Wilmington, DE, USA), talc (Luzenac Pharma M; Imerys, Paris, France), simethicone (Silfar SE 4; Wacker Chemie, Munich, Germany), glycerol (Carl Roth GmbH, Karlsruhe, Germany), calcium silicate (Florite PS-10; Tomita, Naruto, Japan), calcium silicate (Rxcipients®; Evonik, Darmstadt, Germany), mannitol (Pearlitol 25C; Roquette, Lestrem, France), pregelatinized maize starch (Starch 1500; Colorcon, Harleysville, PA, USA), sodium decanoate/sodium caprate (C10) (Biospectra, Bangor, PA, USA), sodium octanoate/sodium caprylate (C8) (Biospectra, Bangor, PA, USA), and medium-chain triglycerides (MCTs) (Miglyol 812 N; IOI Oleo, Hamburg, Germany). Polyoxylglycerides (Labrasol® ALF) were kindly provided by Gattefossé (Saint-Priest Cedex, France) and are treated here as a commercial multicomponent surfactant/solubilizer mixture. Eudracap® Enteric capsules (Figure A1a) used for the encapsulation of the microtablets were kindly provided by Evonik (Darmstadt, Germany). Demineralized water was used for all formulations and solutions.

For dissolution testing, hydrochloric acid from Carl Roth GmbH, Karlsruhe, Germany, and trisodium phosphate dodecane hydrate from TH Geyer, Renningen, Germany, were used.

For HPLC measurements, ammonia (25%) and phosphoric acid (TH Geyer, Renningen, German), HPLC-grade acetonitril (Carl Roth GmbH, Karlsruhe, Germany) and trifluoracetic acid (Avantor, Radnor, PA, USA) were used.

Rybelsus® (14 mg) was obtained from a pharmacy.

2.2. Preparation of Printing Pastes

All pastes were prepared using a Topitec® Touch mixing system with a disk stirrer supplied by WEPA Apothekenbedarf GmbH (Hillscheidt, Germany) in a 150 mL Topitec mixing jar. Prior to the addition of the peptide drug substance (LG/SG), the mixtures were stirred at 500 rpm for 5 min, followed by 300 rpm for 10 min. After the addition of LG/SG, the pastes were further mixed at 300 rpm for 5 min. A "printing paste" denotes a semisolid/viscoelastic feed material (physically a suspension) containing an API, excipients, and liquid vehicle, with flow and shape-retention properties suitable for transfer through a screen or stencil apertures during layer-by-layer printing [39]. All formulations are presented in respective Tables.

The pastes were prepared at room temperature (RT) according to the respective formulations, which are presented in the Results section. Briefly, the binder solutions (Benecel K4M 4% and Klucel LF 10%) were prepared using a Heidolph Scientific Products GmbH (Schwabach, Germany) Hei-TORQUE Ultimate laboratory stirrer. The required amount of water was transferred into a glass beaker. Water heated to 80 °C was used for Benecel K4M, whereas water at RT was used for Klucel LF. The corresponding amount of binder was added while stirring at 400 rpm. Subsequently, the mixtures were homogenized and stirred for 50 min (Benecel K4M) and 20 min (Klucel LF), respectively, at 800 rpm. The binder gels were allowed to rest for 24 h before being used for paste preparation to ensure complete development of the gel network.

2.3. Three-Dimensional Screen and Stencil Printing of Conventional Size and Microtablets Using SPID® Technology

The tablets were manufactured using a prototype lab-scale 3DSP unit, XHS STS 3D (Exentis Group AG, Stetten, Switzerland). Conventional-size tablets, T1 (14 × 5 mm) and T2 (1 × 1 mm), were printed using a screen with a mesh size of 240 µm (Figure A2). As described in [39], screen printing involves the dispersion of a paste (water-based suspension) across a printing screen with a squeegee in a way that gets it into the mesh openings. In a second step, the mesh is pressed with the printing squeegee towards the printing plate. The resulting forces lower the paste's viscosity, allowing capillary forces to transfer the paste to the printing plate at the position of the mesh openings. Once transferred, no further forces are applied to the paste, and given its viscosity characteristics the paste remains in place. Printer settings for T1 and T2 were as follows: flooding and printing squeegee speed: 100 mm/s, off-contact distance: 2 mm, height increment for screen elevation: 15.9 µm, dry temperature: 35 °C, drying time per layer: 20 s.

For the microtablets T3, T4 and T5 (1 × 1 mm), the 3DSP process was varied to use a stainless-steel stencil with an opening size of 1 mm (Figure A2) and a thickness of 60 µm instead of a conventional woven screen. Stencils do not allow for an inner architecture of an object that is being produced but they allow higher flexibility towards excipients and shorter printing times. The stencil-printing process, spatially defined paste transfer to the printing plate and drying, is largely comparable to screen printing. In contrast to screen printing, the paste is brought into the stencil openings, which also transfers it to the printing plate or the top of the previously deposited layer in the same step. The primary reason for using the stencil technique was to allow for reliable printing of paste formulations containing high proportions of surfactant-based permeation enhancers, such as sodium caprate. Printer settings were as follows: printing squeegee speed: 30 mm/s, off-contact distance: 0 mm, height increment for screen elevation: 15 µm, dry temperature: 35 °C, drying time per layer: 30 s.

2.4. Assessment of LG and SG Secondary Structure by Circular Dichroism Spectroscopy

To assess the secondary structure of LG as a model peptide following incorporation into the printed dosage form, circular dichroism (CD) spectroscopy was performed. The LG-containing tablet, T1 (5 mg LG), was dissolved in 1 mL of water, and the resulting solution was diluted 1:10 with water to obtain a final peptide concentration of 0.44 mg/mL. For comparison, an LG reference solution was prepared in water at a concentration of 0.4 mg/mL, either in the presence or absence of a dissolved placebo tablet.

Far-UV CD spectra were recorded at 20 °C using a Jasco J-810 spectropolarimeter (JASCO Corporation, Hachioli, Tokyo, Japan) and a cuvette with an optical path length of 0.1 mm. Measurements were performed at a pH of 7–8, with the instrument voltage maintained below 600 V. Each spectrum was obtained by averaging 60 consecutive scans and corrected by subtracting the corresponding background spectrum. The same procedure was used for SG. However, due to the presence of triglycerides, an additional centrifugation step was necessary.

2.5. Characterization of Microtablets Based on Their Mass and Dimensions

The individual mass of 100 microtablets (T5) was determined using an analytical balance (Mettler Toledo, Columbus, OH, USA). Subsequently, the dimensions, such as the height and diameter, of each microtablet were evaluated using a digital microscope (VHX-X1; Keyence Corporation, Osaka, Japan) equipped with a Fully-Integrated (FI) Head VHX-7100 and different lenses (VHX-E-00, VHX-E-20, and VHX-E-100). Image acquisition,

three-dimensional reconstruction and dimensional measurements were performed with the VHX Control System software (Ver. 23.11.16.0A (2.0)).

Each printed microtablet ($n = 100$) was imaged at a magnification of 150×. The minimum and maximum diameters were determined using the integrated software tool "Automatic Area Measurement/Count" of the microscope. Each tablet was repositioned three times, resulting in three replicate measurements per tablet ($n = 3$).

For the height measurements, three-dimensional images of the tablets were obtained with the 3D depth composition function of the microscope. The resulting 3D images were used to generate height profiles along horizontal and vertical directions. For each tablet, three profiles were evaluated in each orientation, and the maximum height was determined from each profile to reduce the influence of individual profile selection on the determined tablet height.

Measurement data were exported from the VHX Control System software (Ver. 23.11.16.0A (2.0)) and further processed in Microsoft Excel LTSC 2024 (version 2408, build 16.0.17932.20910; Microsoft Corporation, Redmond, WA, USA). Unless stated otherwise, results are presented as the mean ± standard deviation (SD) of $n = 3$ per tablet.

2.6. Filling Microtablets into Capsules

Based on the uniform active pharmaceutical ingredient (API) loading of 5% (w/w) in all LG- and SG-containing microtablets, approximately 300 mg of microtablets was filled into each capsule to achieve a target dose of 15 mg API per capsule (Table A1). All LG-containing microtablets (T2, T3 and T4), as well as the SG-containing microtablet T5, were filled manually with the help of a ProFunnel Kit (#000-5), Profill (TORPAC, Fairfield, NJ, USA) into Eudracap® Enteric Size 0 capsule (Figure A1), which tools were kindly provided by Evonik, Darmstadt, Germany.

2.7. In Vitro Dissolution Testing of LG and SG Tablets and Microtablets Contained in Enteric Capsules

The dissolution profiles of the LG-containing formulations (T1, T2, T3, and T4) were determined using a paddle apparatus (USP Apparatus II) equipped with an automated sampling station (Agilent Technologies, Santa Clara, CA, USA), which was used to collect samples at predefined time points. The test was started with 750 mL of 0.1 M HCl as the dissolution medium. Two tablets of T1, three capsules each of T2 and T3, and one capsule of T4 were tested. Each capsule/tablet was placed in a spiral-coated capsule sinker to prevent flotation and ensure complete immersion throughout the dissolution experiment. T1 was tested in 0.1 M HCl for 30 min at 37.5 °C and 50 rpm, with samples collected at 0, 5, 10, 15, 20, 25 and 30 min. The capsules were initially incubated in 0.1 M HCl for 2 h at 37.5 °C and 50 rpm to simulate passage through the stomach. Subsequently, the dissolution medium was adjusted to pH 6.85 by the addition of trisodium phosphate (Na_3PO_4) solution to simulate the intestinal environment. The pH was verified using a pH meter (Mettler Toledo, Columbus, OH, USA). Dissolution testing of the capsules was then continued for an additional 1.5 h, resulting in a total test duration of 3.5 h. Samples were collected at 120, 135, 150, 157.5, 165, 180 and 210 min. At each sampling time point, 1 mL of dissolution medium was withdrawn for analytical determination. The reduction in media volume due to sampling was taken into account for the drug-release calculations.

The dissolution profile of the semaglutide-containing microtablet formulation T5 was determined using a flow-through UV–Vis dissolution system. Each enteric capsule was placed in a rotating basket within an individual dissolution vessel containing pH 6.8 phosphate buffer (Ph. Eur.) maintained at 37.5 °C. The rotating baskets were operated at

50 rpm. Drug release was monitored at 205 nm. The empty capsule as well as the placebo microtablets were also measured and subtracted from the measurement.

2.8. High-Performance Liquid Chromatography (HPLC) for LG-Containing Dissolution Samples

LG was quantified by HPLC using a diode array detector set at 280 nm. Separation was performed on a 100 mm × 2.1 mm, 1.7 µm CSH C18 column (Waters, Frankfurt am Main, Germany) maintained at 12 °C. The injection volume was 3 µL. Mobile phase A consisted of 10% acetonitrile (ACN) and 0.1% trifluoroacetic acid (TFA), whereas mobile phase B consisted of 80% ACN and 0.1% TFA in water. The mobile-phase gradient is presented in Table A2.

A stock solution of LG (0.3 mg/mL) was prepared in ammonium phosphate buffer (pH 8.0) and ACN at a ratio of 2:1 (*v*/*v*). Standard and calibration solutions containing 0.015 mg/mL LG were prepared in the same solvent mixture. For the dissolution testing, 1 mL samples were withdrawn at the respective sampling time points and analyzed by HPLC. All solutions were protected from light and stored at 5 °C until injection into the chromatograph.

2.9. In Vivo Pig Study

The pharmacokinetic study was done in collaboration with the University of Veterinary Medicine Vienna, University Clinic for Swine, Vienna, Austria, for the in vivo part. Permission for the study was granted by the institution's Animal Welfare Committee (ETK 104/10/2024). Six experimental groups were investigated, comprising four LG groups (T1, T2, T3 and T4) and two SG groups (T5 and Rybelsus). T1 was administered at a dose of 5 mg LG, whereas T2, T3, and T4 were administered at a dose of 15 mg LG. T5 and Rybelsus® were administered at a dose of 15 and 14 mg SG, respectively. T1 and Rybelsus® were conventional-size tablets, whereas T2, T3, T4, and T5 were capsules, specifically Eudracap® Enteric capsules (size 0), containing the microtablets.

For the endoscopic application of the dosage forms directly into the stomach using a gastroscope (Olympus, Shinjuku, Japan), the study animals (n = 4/group for LG and 3/group for SG) were kept without straw bedding for 48 h and were fasted for 24 h before being anesthetized (0.5 mg/kg body weight (bw) azaperone and 10 mg/kg bw ketamine intravenously or 2 mg/kg bw azaperone and 25 mg/kg bw ketamine intramuscularly). To determine the pharmacokinetic profile of the LG/SG dosage forms, blood samples (maximum blood volume per time point: 2 mL) were collected shortly before application of the tablets (time point: 0 h) and at predefined time points after administration by puncturing the vena cava cranialis or vena jugularis with 21G needles. For the formulations T2-T5, blood samples were collected at 30, 60, 90, 180, 240, 360, 480 min, and 24 h. For the reference tablet Rybelsus®, blood samples were collected at 0, 120, 240, 420, 600 min, 24, 32 and 48 h. Plasma samples were frozen and stored at −80 °C until analysis. Pigs had to be older than 6 weeks and weigh less than 25 kg. The mean weight was 15.8 ± 2.4 kg.

2.10. Measurement of LG and SG Plasma Levels

Plasma LG concentrations were quantified by Liquid Chromatography–High-Resolution Mass Spectrometry (LC-HRMS) using a Thermo Fisher (Thermo Fisher Scientific, Waltham, MA, USA) system with a Vanquish pump system and an Autosampler coupled to a Q-Exactive orbitrap mass spectrometer equipped with a heated electrospray ionization source (H-ESI2). Separation was performed on a Premier Peptide CSH-C18 column (150 × 2.1 mm, 2.6 µm; Waters, Milford, MA, USA) equipped with a C6-Phenyl guard column using a gradient of 0.1% formic acid in ACN (mobile phase A) and 0.1% formic acid in water (mobile phase B) at a flow rate of 0.25 mL/min. Mass spectrometric detection was performed in

positive ionization mode using parallel reaction monitoring (PRM). The monitored ions and MS source parameters are summarized in Table A3.

Plasma samples were prepared by protein precipitation using methanol and purified by solid-phase extraction. Briefly, 80 µL of plasma was mixed with an internal standard (d-liraglutide) and subjected to protein precipitation with methanol. Following centrifugation, the supernatant was purified using Oasis MAX µ-elution plates, evaporated, and reconstituted in acetonitrile (ACN)/water containing 5% formic acid.

Plasma SG concentrations were quantified by LC-HRMS coupled with Tandem Mass Spectrometry (HPLC-MS/MS) on a Q-Exactive Orbitrap mass spectrometer coupled to an Ultimate 3000 RS UHPLC system (Thermo Fisher Scientific, Waltham, MA, USA) equipped with an Accela Open Autosampler. Chromatographic separation was achieved on a Jupiter C18 column (150 × 2 mm, 5 µm; Phenomenex, Torrance, CA, USA) using a gradient consisting of 0.1% formic acid in ACN (mobile phase A) and 0.1% formic acid in water (mobile phase B) at a flow rate of 0.60 mL/min. The injection volume was 4 µL. Mass spectrometric detection was performed using heated electrospray ionization (H-ESI) in positive ion mode with MS/MS acquisition. The available mass spectrometric parameters are summarized in Table A4.

Plasma samples were prepared by protein precipitation with methanol. Briefly, 80 µL of plasma was mixed with 20 µL of working solution and 20 µL of internal standard (dioclofenac), followed by the addition of 240 µL methanol. After centrifugation, the supernatant was transferred, mixed with 10% ammonia solution, evaporated to dryness under a nitrogen stream, and reconstituted in acetonitrile/water containing 5% formic acid.

2.11. Data Analysis and Visualization

Figure 1 was created using Microsoft® PowerPoint, Version 2508 (Microsoft Corporation, Redmond, WA, USA). Graphical visualization of the in vitro drug release and pharmacokinetic data was performed using OriginPro 2026, Version 10.3.0.197 (OriginLab Corporation, Northampton, MA, USA). For graphical presentation of the pharmacokinetic data, mean plasma concentrations were calculated across all animals within each group ($n = 3$ or 4) at each sampling time point and subsequently plotted. Pharmacokinetic parameters, including Area Under the Curve from 0 to the time of the last quantifiable concentration (AUC_{last}) of T1-T5, were calculated from the individual animal data using Origin Pro (Version 10.3.0.197).

2.12. Statistical Analysis

To assess a potential correlation between microtablet size and mass, Pearson's r was calculated from linear fitting of the complete dataset ($n = 100$) using Origin Pro (Version 10.3.0.197). Statistical significance was assessed using a two-tailed *t*-test.

To compare groups regarding peptide absorption, the AUC_{last} values of individual animals were compared. Plasma concentrations below the lower limit of quantification (LLOQ liraglutide: 1.5 ng/mL, LLOQ semaglutide: 1.0 ng/mL) were imputed as one half of the LLOQ (liraglutide: 0.75, semaglutide: 0.5) prior to pharmacokinetic analysis. AUC_{last} values were calculated for each animal using the linear trapezoidal rule. AUC_{last} values were log-transformed prior to statistical analysis. Group differences were assessed using Welch's *t*-test, which does not assume equal variances between groups. Test results were not adjusted by multiplicity, and statistical significance was defined as $p < 0.05$.

3. Results

3.1. Testing a Tablet of Conventional Size and Format

In our effort to develop injection-free GLP-1-RA alternative dosage forms, we first tested a conventionally sized tablet format. We used an immediate-release-type paste

matrix containing a well-established permeation enhancer, sodium caprate (C10), and LG at a 1:5 weight ratio (LG) to manufacture oval tablets (size: 14 mm × 5 mm × 2 mm; Figure 1) employing the 3DSP/SPID® technology [39]. The composition of the paste is shown in Table 1. This formulation offered good printability. Physicochemical evaluation of resulting tablets demonstrated that they comply with regulatory requirements (Table A5). In vitro dissolution studies confirmed the rapid drug release. Approximately 55% of the LG was released after 10 min, with over 90% released after 20 min and almost complete release by 30 min (Figure 1b). It is important to note that the formulation and printing process did not appear to jeopardize the integrity of LG as assessed with circular dichroism (CD) spectroscopy (Figure A5a).

Table 1. Formulation of the conventional-size, oval LG tablet T1.

		T1		
		Oval Tablet		
No.	**Ingredients** [a]	**Function**	**wt% Paste**	**wt% Tablet** [b]
1	Liraglutide	API	1.71	5.17
2	Low-substituted HPC (L-HPC LH-31)	Binder	10.13	30.71
3	MCT (Miglyol 812 N)	Humectant	0.85	2.57
4	Calcium silicate (RxCIPIENTS®)	Adsorbent	1.36	4.13
5	Simethicone (Silfar SE 4)	Anti-Foaming Agent	1.30	3.95
6	Sodium Caprate (C10)	Permeation Enhancer	16.51	50.06
7	Talc (Luzenac Pharma M)	Anti-Tacking Agent	1.13	3.41
8	Water	Solvent	67.01	-
	Total		100.00	100.00

[a] Chemical name (trade name), [b] dried mass.

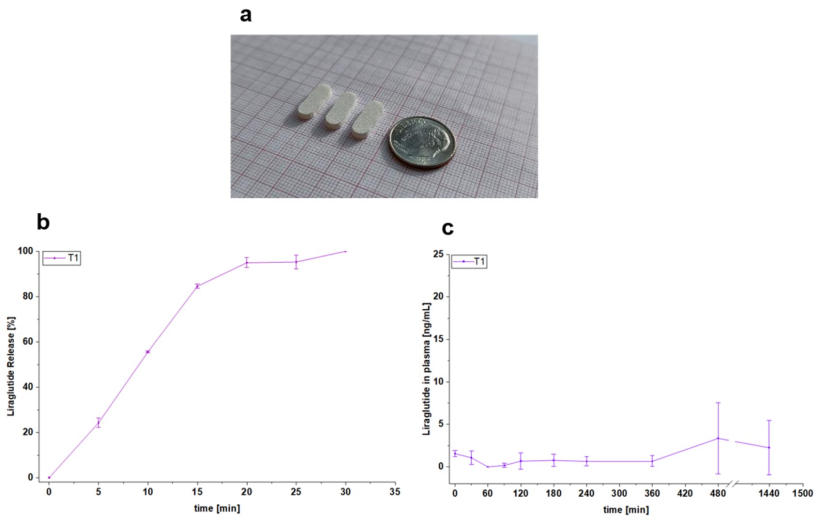

Figure 1. Characterization of the conventional-size oval LG tablet T1. (**a**) Photograph of 3 tablets. (**b**) In vitro release profile of the tablets in a 0.1 M HCl solution (pH 1.2) for 30 min. (**c**) LG plasma concentrations in 24 h pharmacokinetic study in pigs. The data are presented as mean ± SD, $n = 3$.

When subjected to in vivo studies in pigs, administration of the T1 tablets did not result in significant LG blood levels (Figure 1c). Plasma levels remained close to the lower quantifiable range during the first 6 h, with only a slight increase observed at 480 min before declining again at 24 h.

3.2. Switching to the Microtablet Format Enabled by SPID®

There are several factors that may have contributed to the low bioavailability of LG in T1. Our aim was to overcome critical issues such as degradation in the acidic environment of the stomach and the relatively slow drug release from the large tablet format. To this end, we have developed a new dosage format that combines the strengths of SPID® with those of conventional drug manufacturing tools (Figures A2 and A3). Specifically, we designed a dosage form that integrates 3DSP microtablets into enteric capsules. The microtablet format (Figure 2) was chosen to speed up drug release, as its higher surface area-to-volume ratio (SA/V) enables quicker release. According to the Noyes–Whitney and Nernst–Brunner equations, the dissolution rate is directly proportional to the surface area exposed to the dissolution medium; consequently, increasing the SA/V accelerates tablet dissolution and drug release. This relationship was confirmed by comparing a conventional oval-shaped tablet (14 × 5 × 1.5 mm; SA/V = 1.85) with SPID®-printed cylindrical microtablets (diameter: 0.9 mm, height: 0.9 mm; SA/V = 6.67), as the microtablets exhibited substantially faster drug release (Figure A4 and [40–43]).

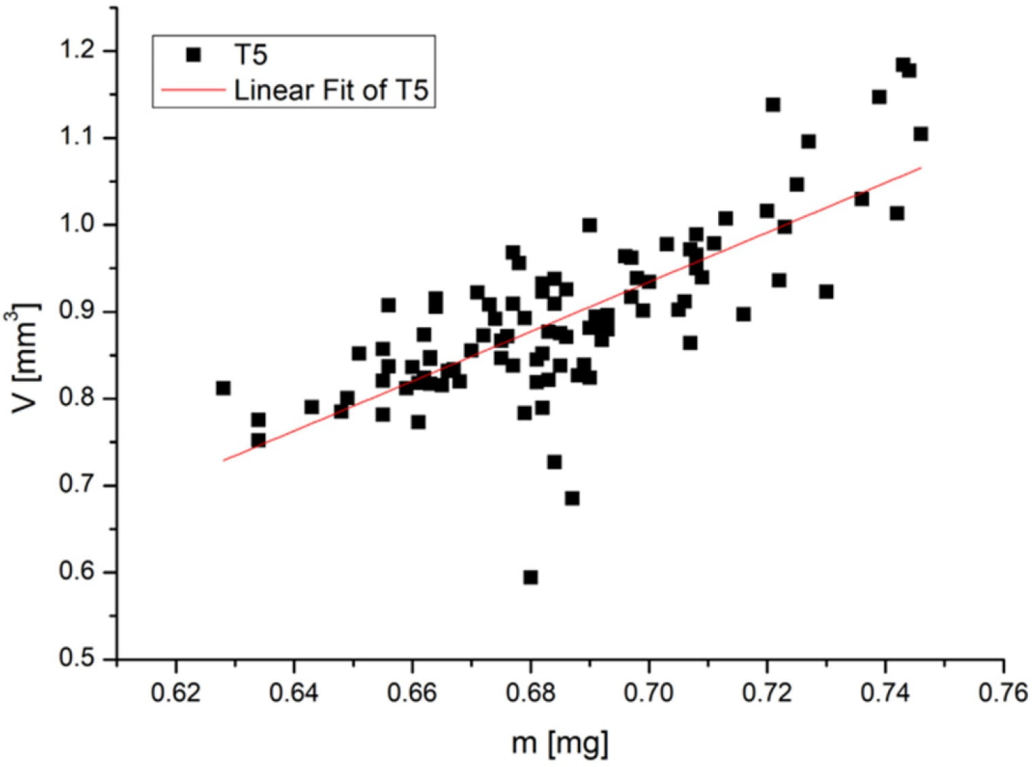

Figure 2. Correlation between the mass of individual T5 microtablets and their calculated volume (mm^3). Microtablet volume was calculated from the measured diameter and height, assuming a cylindrical geometry. Dimensions of individual microtablets were determined using a digital microscope and VHX Control System software. Each data point represents one microtablet. A strong positive correlation was observed (Pearson's r = 0.75185, $R^2 = 0.56084$, $p < 0.001$, $n = 100$).

Having designed the new dosage format, we had to demonstrate the feasibility of reliably printing microtablets containing surfactant-based permeation enhancers. To this end, we varied conventional 3DSP to use a stencil instead of a printing screen. With stencils,

printing paste is transferred through the openings of the stencil onto the printing plate or on top of the previous layer. Due to its viscoelastic characteristics, the paste remains in place when the plate is lowered and moved to the drying station. Once the layer has been dried, the cycle continues with the addition of the next layer of paste. Stencil printing is based on the same underlying physicochemical principles. It is not limited by the size of particles within the paste and allows for more flexibility towards excipients, thicker layers and quicker processing time.

To get an understanding of the uniformity of the microtablets, we assessed their mass and dimensions. A total of 100 randomly selected T5 microtablets were weighed and their dimensions (diameter and height) were obtained using a microscope-based approach. The mass and volume distribution of the 100 tablets are summarized in Table 2 and Figure 2. Their mean mass was 0.686 mg ± 0.026 mg, corresponding to a Relative Standard Deviation (RSD) of 3.73%. Their mean diameter was 1.190 ± 0.053 mm (RSD = 4.42%). Their mean height was 0.801 ± 0.031 mm (RSD = 3.92%). These data demonstrate the high uniformity of the T5 microtablets. We next assessed the relationship between the mass and volume of the microtablets (Figure 2). There was a strong and significant positive correlation between the mass and volume of the microtablets (Pearson's r = 0.75185, $R^2 = 0.56084$, $p < 0.001$, $n = 100$), adding another aspect of reproducibility.

Table 2. Mass and dimensional characteristics of SG T5 microtablets, expressed as mean, SD, and relative standard deviation (RSD).

T5	Sample Size (n)	Mean	SD	RSD
Mass [mg]	100	0.686	0.026	3.73%
Diameter [mm]	100	1.190	0.053	4.42%
Height [mm]	100	0.801	0.031	3.92%

The morphology of the microtablets (T5), based on microscopic pictures of a representative microtablet, is shown in Figure 3. The tablet is shown vis-à-vis a 2 Euro Cent coin to put it into perspective as well as from the top and side. The surface is plain. The side view reveals minor irregularities.

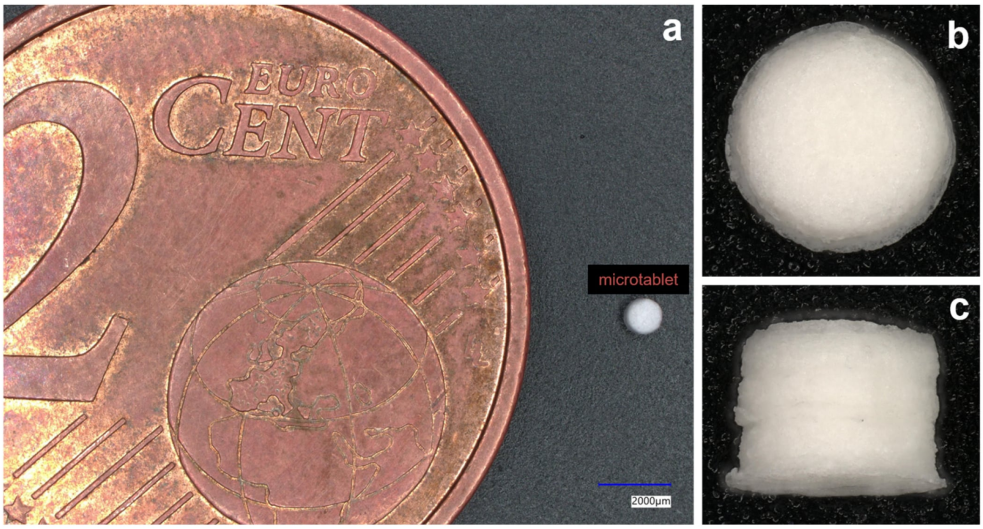

Figure 3. Microscopic images of a SPID®-printed microtablet T5. (**a**) Size comparison of the microtablet with a 2-cent euro coin (scale bar: 2000 µm). (**b**) Magnified top view showing the circular tablet geometry and surface morphology. (**c**) Magnified side view illustrating the microtablet thickness and structural appearance.

Results obtained confirm the uniformity of the microtablets. To protect the peptides from degradation in the stomach, the microtablets were placed in enteric capsules. The Eudracap® Enteric capsules used are designed to dissolve at a pH of 6.85, thus delivering their contents to the small intestine. To this end, microtablets were manually filled into the enteric capsules with the help of the ProFunnel Kit (#000-5), Profill. Capsules were filled with microtablets based on their weight; a total of 300 mg of microtablets, representing an LG and SG dose of 15 mg, was filled into each capsule. This dose is similar to the SG content of the 14 mg Rybelsus® tablet.

3.3. Applying the Microtablet/Capsule Format to LG Formulations

We tested a series of microtablets (T2 tablets were produced by screen printing, and T3 and T4 were produced by stencil printing) differing primarily in terms of the permeation enhancer.

The reference, T2, was formulated without a permeation enhancer and was based on HPC. In formulations T3 and T4, HPC was replaced by HPMC to ensure the intact release of the microtablets from capsule shells and, consequently, their uniform distribution in the small intestine. While T3 contained C10 as the sole permeation enhancer, T4 contained a combination of sodium caprate (33.3%) and sodium caprylate (16.7%). All formulations for LG-containing microtablets are summarized in Table 3.

The resulting microtablets were placed into enteric capsules according to weight. Each capsule was filled with 300 mg of microtablets (Table A1). Based on the designed API load of 5% (*w*/*w*), the capsules were expected to contain 15 mg of LG each.

The drug release of all three formulations was tested in in vitro dissolution studies (Figure 4). No LG was released during the first 120 min when the conditions were acidic. This confirmed that the enteric capsule was intact and that the formulation was effectively protected against premature drug release. Following the pH shift to 6.85, all formulations exhibited rapid drug release. T2 showed the fastest dissolution, reaching approximately 50% cumulative release within 30 min after the pH shift and more than 90% after 50 min. T3 and T4 released LG somewhat slower due to the use of HPMC instead of HPC. Among these, T4 released LG slightly more rapidly than T3, reaching approximately 70% release after 60 min compared with about 60% for T3. Complete drug release was achieved for all formulations within 90 min after the pH shift. It should be noted that for T4 only one capsule filled with microtablets was measured due to limited availability.

Table 3. The compositions of the 3DSP pastes and the corresponding microtablet formulations of T2, T3 and T4.

		T2		**T3**		**T4**	
		Without PE		**With C10**		**With C10 and C8**	
Function	**Ingredients** [a]	**wt% Paste**	**wt% Tablet** [b]	**wt% Paste**	**wt% Tablet** [b]	**wt% Paste**	**wt% Tablet** [b]
API	Liraglutide	2.83	5.00	1.81	5.00	1.80	5.00
Permeation Enhancer	Sodium caprate (C10)			18.10	50.00	12.05	33.30
Permeation Enhancer	Sodium caprylate (C8)					6.05	16.70
Binder	HPC (Klucel LF Pharma)	2.35	4.14				
Binder	HPMC (Benecel K4M)			1.17	3.23	1.17	3.23

Table 3. *Cont.*

		T2		T3		T4	
		Without PE		With C10		With C10 and C8	
Function	**Ingredients** [a]	**wt% Paste**	**wt% Tablet** [b]	**wt% Paste**	**wt% Tablet** [b]	**wt% Paste**	**wt% Tablet** [b]
Anti-Foaming Agent	Simethicone (Silfar SE 4)	0.09	0.15	1.44	3.97	1.44	3.97
Anti-Tacking Agent	Talc (Luzenac Pharma M)	0.78	1.37	1.25	3.44	1.25	3.44
Filler	Calcium silicate (Florite PS-10)	2.96	5.23	1.86	5.16	1.87	5.16
Filler	Mannitol (Pearlitol 25C)	43.63	77.06	2.40	6.62	2.40	6.62
Filler	MCC (Avicel PH-105)			5.07	14.00	5.07	14.00
Filler	Pregel. maize starch (Starch 1500)			0.73	2.00	0.73	2.00
Humectant	Glycerol	2.72	4.83	1.45	4.00	1.46	4.00
Humectant	MCT (Miglyol 812 N)	1.26	2.22	0.94	2.58	0.93	2.58
Solvent	Water	43.38	-	63.79	-	63.82	-
	Total	100.00	100.00	100.00	100.00	100.00	100.00

[a] Chemical name (trade name), [b] dried mass.

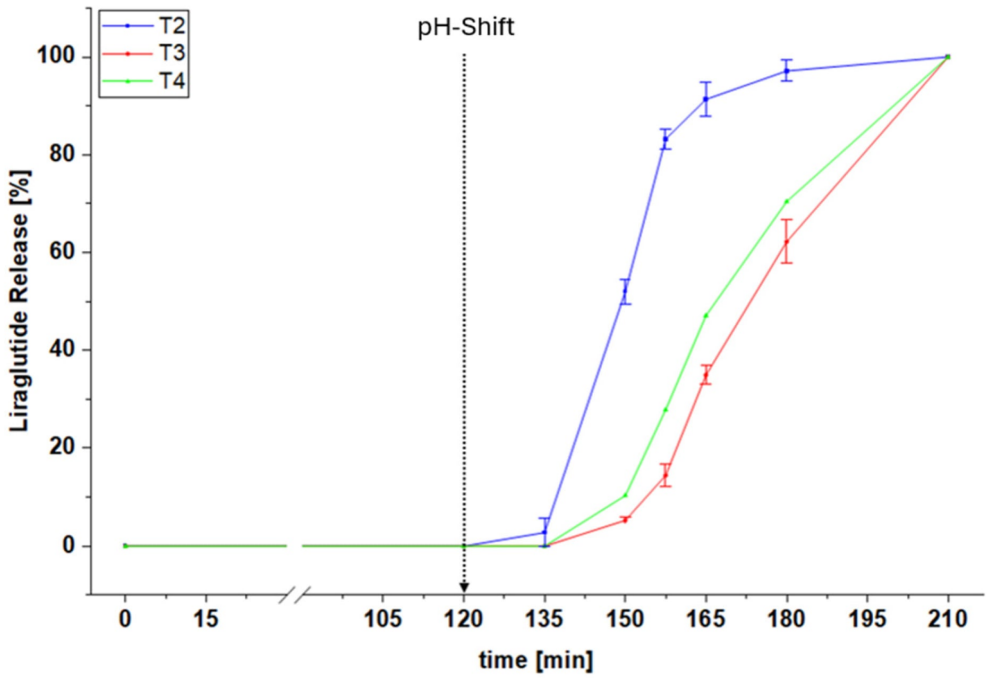

Figure 4. Release profiles of the LG-containing microtablets, T2, T3 and T4, filled into enteric capsules (Eudracap® Enteric, pH = 6.2) in 0.1 M HCl solution (pH 1.2) for 120 min, followed by an additional 90 min in neutral medium (pH 6.85). The data are presented as the mean ± SD of relative LG release, $n = 3$ (T2 and T3) and $n = 1$ (T4).

3.4. The Microtablet/Enteric Capsule Concept Greatly Increases Bioavailability of LG

Next, we tested the three new dosage forms in vivo. They were administered to the stomachs of fasted pigs, and LG blood levels were measured regularly over a period of 24 h. Compared to the reference formulation (T2), which contained LG but no permeation enhancer, formulations containing a single permeation enhancer, C10 (T3), or a combination of C10 and C8 (T4) yielded markedly higher systemic exposure (Figure 5 and Table 4). T3 reached the highest plasma concentration (c_{max} = 10.9 ± 4.9 ng/mL) at approximately 210 min, and T4 exhibited its maximum concentration (c_{max} = 11.6 ± 6.1 ng/mL) at approximately 300 min. T3 exhibited the highest overall exposure with an AUC_{last} of 132.92 ± 114.17 ng·h/mL, followed by T4 (115.85 ± 62.07 ng·h/mL). In contrast, the reference formulation, T2, without a permeation enhancer showed only limited systemic exposure (c_{max} = 1.9 ± 2.7 ng/mL, AUC_{last} = 32.17 ± 45.50 ng·h/mL). Compared to the reference, T2, the bioavailability measure, AUC_{last}, was 4.1-fold and 3.6-fold higher for T3 and T4, respectively.

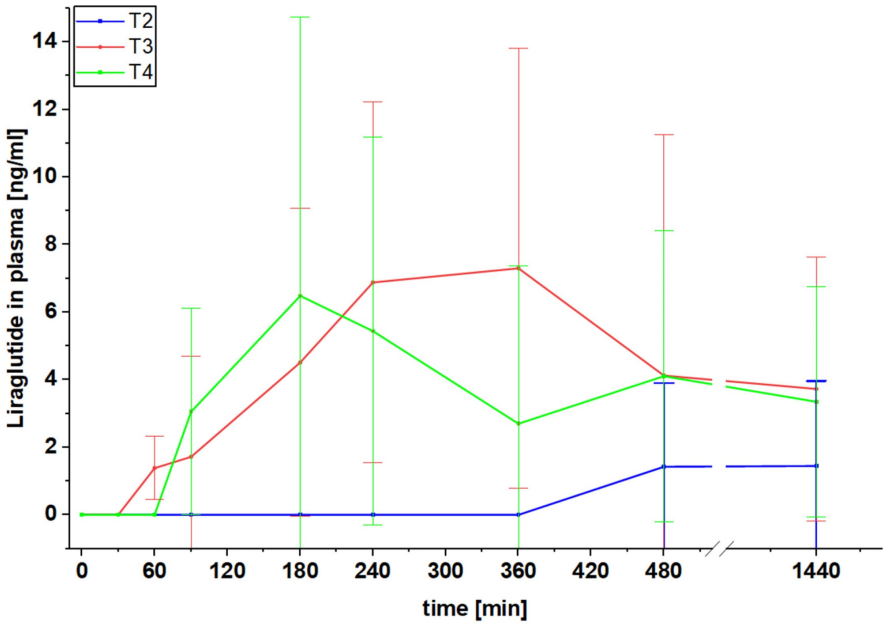

Figure 5. Mean plasma concentrations of LG-containing microtablets, T2, T3 and T4, filled into enteric capsules (Eudracap® Enteric, pH = 6.2) in a 24 h pharmacokinetic study in pigs. LG plasma concentrations are presented as mean ± SD, n = 4. Statistical analysis demonstrated a significant difference for AUC_{last} between T4 and T2, p = 0.0276, and a trend for T3 vs. T2, p = 0.0857.

Table 4. Pharmacokinetic parameters of the LG-containing microtablets, T2, T3, and T4, in capsules, including mean observed time to maximum plasma concentration (t_{max}) and mean maximum concentration (c_{max}), as well as calculated Area Under the Curve from 0 to the time of the last quantifiable concentration (AUC_{last}) with standard deviation (SD).

Tablet	t_{max}	c_{max}	AUC_{last}	Dose	F_{rel}
	[min]	[ng/mL]	[ng·h/mL]	[mg]	[%]
T2	1440 *	1.9 ± 2.7 *	32.17 ± 45.50	15.00	100
T3	210 ± 112	10.9 ± 4.9	132.92 ± 114.17	15.00	413
T4	300 ± 129	11.6 ± 6.1	115.85 ± 62.07	15.00	360

Pharmacokinetic parameters were observed/calculated based on the mean plasma concentration-time profiles of each treatment group (n = 4). Calculations were performed using OriginPro (Version 10.3.0.197). * In one animal, LG concentrations were measured towards the end of the 1440 min observation period.

3.5. Microtablet/Enteric Capsule Concept Translated to SG

Next, we were interested in testing whether the microtablet/enteric capsule concept could be applied to another GLP-1-RA. SG-containing microtablets were produced according to the formulation shown in Table 5. In the case of SG, we used a combination of a permeation enhancer and a solubilizer: C10 was selected as the permeation enhancer because it is one of the most extensively investigated medium-chain fatty acids and has been shown to transiently open tight junctions, reduce transepithelial electrical resistance (TEER), and thereby enhance the paracellular transport of peptide drugs across the intestinal epithelium [29,34,44–46]. Labrasol® ALF, a non-ionic surfactant, was included as a solubilizer, which can self-assemble into micellar structures in aqueous environments that associate with drug molecules and maintain them in a solubilized state [47–49]. This may provide an additional formulation benefit for the poorly soluble peptide SG. The dissolution behavior of SG in T5 is shown in Figure A6. Complete dissolution was slower for the SG formulation (180 min) compared with the LG dosage forms, T3 and T4 (90 min). Additionally, the integrity of SG was investigated with CD spectroscopy. Figure A5 revealed evidence that the integrity of the peptide did not differ compared to a fresh SG solution. Moreover, storing microtablets for 6 months at room temperature did not change the spectroscopy profile, suggesting the molecular integrity of SG.

Table 5. The compositions of the 3DSP pastes and the corresponding microtablet formulation of T5.

		T5	
		With C10 and Labrasol	
Function	**Ingredients** [a]	**wt% Paste**	**wt% Tablet** [b]
API	Semaglutide	1.81	5.00
Permeation Enhancer	Sodium Caprate (C10)	9.04	25.00
Binder	HPMC (Benecel K4M)	1.17	3.23
Anti-Foaming Agent	Simethicone (Silfar SE 4)	1.44	3.97
Anti-Tacking Agent	Talc (Luzenac Pharma M)	1.25	3.44
Filler	MCC (Avicel PH-105)	8.28	22.91
Filler	Calcium silicate (Florite PS-10)	1.87	5.16
Filler	Mannitol (Pearlitol 25C)	5.07	14.02
Filler	Pregel. maize Starch (Starch 1500)	1.18	3.27
Humectant	Glycerol	1.44	4.00
Solubilizer	Polyoxylglycerides (Labrasol® ALF)	3.60	10.00
Solvent	Water	63.85	-
Total		100.00	100.00

[a] Chemical name (trade name), [b] dried mass.

Figure 6 and Table 6 summarize the pharmacokinetic profiles of SG following oral administration of formulation T5 and the reference product, Rybelsus®. Compared with Rybelsus®, T5 exhibited higher plasma concentrations over the entire observation period and resulted in improved oral bioavailability. T5 achieved a c_{max} of 18.5 ± 23.02 ng/mL

with a dose-normalized AUC_{last} of 139.68 ± 165.97 ng·h/mL, compared with a c_{max} of 0.98 ± 1.39 ng/mL and a dose-normalized AUC_{last} of 13.87 ± 19.61 ng·h/mL for Rybelsus®. Pharmacokinetic parameters were calculated from the individual animal plasma concentration–time profiles of each treatment group ($n = 3$). The average AUC_{last} value was 10.07 times higher in the T5 versus the Rybelsus® arm, resulting in a dose-normalized relative bioavailability of 940% for T5. These results demonstrate the potential of such novel dosage forms to enhance systemic exposure compared with Rybelsus®. Additional studies will have to address the contribution of their individual elements. Statistical analysis was hampered by the small sample size and the observation that only one animal in the Rybelsus® group achieved quantifiable SG AUC_{last} values over the 1440 min observation period. Additionally, one animal in the T5 group had low SG blood levels, potentially qualifying it as an outlier. Nevertheless, the data suggest the potential of the T5 dosage form and warrant further evaluation of this approach, which integrates targeting of specific regions of the intestine and optimizing release properties and formulation.

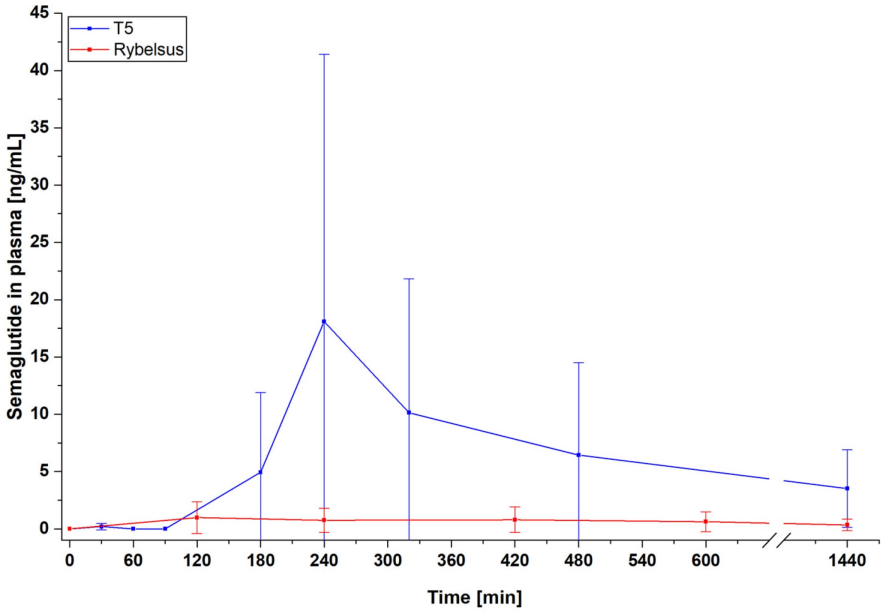

Figure 6. Mean plasma concentrations of SG-containing T5 microtablets filled into enteric capsules and the reference oral dosage form, Rybelsus®, over 2-h in pigs. The administered dose was 15 mg for T5 and 14 mg in the case of Rybelsus. The data are presented as the mean ± SD, $n = 3$ (T5) and $n = 3$ (Rybelsus®). For technical reasons, blood sampling time points were not fully identical for Rybelsus and T5. Statistical comparison of AUC_{last} revealed a p-value of 0.373 between T5 and Rybelsus considering all animals. Removing the outlier animal, T5-2, changed the p-value to 0.202.

Table 6. Pharmacokinetic parameters of the semaglutide-containing T5 microtablets in capsules (15 mg) and Rybelsus® (14 mg). Calculations were performed using OriginPro (Version 10.3.0.197).

Tablet	**Rybelsus**				**T5**			
Dose [mg]	**14**				**15**			
n	**1**	**2**	**3**	**Mean**	**1**	**2**	**3**	**Mean**
c_{max} [ng/mL]	2.94	0	0	0.98 ± 1.39	3.92	0.59	51.00	18.50 ± 23.02
t_{max} [h]	2	-	-	2	6	0.5	4	3.5 ± 2.3
AUC_{last} [h·ng/mL]	41.6	0	0	13.87 ± 19.61	45.84	0.29	372.92	139.68 ± 165.97
F_{rel} [%]	100				940			

4. Discussion

This pilot study demonstrates the feasibility of manufacturing oral dosage forms containing peptides and permeation enhancers using conventional SPID® as well as its variation using a stencil. We tested different concepts enabled by SPID® technology. These included tablets of different sizes, conventional versus microtablets, generated using different permeation enhancers and combinations thereof along with protection from degradation in the stomach. We were able to establish formulations allowing excellent printability. In vivo testing of tablets representing the various concepts showed that microtablets containing the permeation enhancer C10, which were protected from gastric degradation by enteric capsules, yielded superior and promising bioavailability, warranting further development.

Manufacturing conventional tablets containing permeation enhancers such as sodium caprate or SNAC presents challenges related to high enhancer loading, formulation properties, and reproducible tablet performance. Critically, the formulation must maintain spatial and temporal co-localization of the API and enhancer to generate a sufficiently high local enhancer concentration at the absorption surface [25,29,31]. Differences in formulation and dissolution can therefore translate into variability in absorption, while peptide stability and gastrointestinal dilution add further complexity [29,50,51]. These factors contribute to the substantial inter- and intra-subject variability characteristic of many oral peptide formulations.

SPID® is a highly flexible manufacturing technology. This refers to both the tablet geometry/architecture [52] and the compatibility with excipients and APIs [39,52–56]. Both are highly relevant for the production of oral dosage forms of peptide drugs. Rapid release of APIs and permeation enhancers will lead to high local concentrations of both, which is key for the absorption of the peptides. To this end, reducing the tablet size can critically contribute, as release kinetics are controlled, among other things, by the surface-to-volume ratio, with higher ratios being associated with quicker release [40–43]. In addition, a key advantage of SPID® is its broad compatibility with pharmaceutical excipients and API pharmaceutical ingredients. LG and SG were successfully processed into pastes and printed consistently into both conventional-size and microtablets. Of note, circular dichroism spectroscopy of LG and SG demonstrated that the peptides's secondary structure remained unchanged following the 3D screen-printing process, which is consistent with the notion that the printing process does not compromise the molecule's integrity, nor is it likely to compromise its functionality. Moreover, the successful incorporation of high amounts of permeation enhancers, including C10 and C8, demonstrates the capability of SPID® to process formulations that are often challenging for conventional tablet manufacturing due to poor powder flow, compressibility, and tabletability. SPID® is a solvent-based additive manufacturing process. Printing is performed at RT, followed by short drying steps at moderate temperatures (30–70 °C). Compared with fused deposition modeling (FDM), which typically requires elevated processing temperatures, SPID® is particularly suitable for thermolabile excipients and peptide-based drug substances. Collectively, these studies further emphasize the exceptional formulation flexibility of SPID® and its potential as a versatile manufacturing platform for, among other things, oral peptide dosage forms.

The in vivo studies presented here provided an initial proof of concept, showing that SPID® technology can be used to successfully manufacture peptide-based oral dosage forms capable of yielding bioavailability values likely superior to those of current solutions.

Firstly, we investigated the possibility of incorporating LG and a permeation enhancer into conventionally sized and shaped tablets. The resulting SPID® tablets met regulatory requirements. Their bioavailability was evaluated and found to be only moderately higher than that of tablets without a permeation enhancer.

While there exists the possibility that conventional dosage forms containing higher amounts of LG would present with competitive bioavailability, we changed our approach. On the one hand, we wanted to enhance the rate of release by varying the tablet size. On the other hand, we wanted to increase bioavailability through targeted release in the small intestine. To this end, we produced microtablets containing LG and the permeation enhancers C10 and/or C8. We then packaged these microtablets in enteric capsules that release their contents at a pH of 6.85, i.e., in the small intestine. We successfully formulated and printed the appropriate pastes into microtablets. The methods applied, gravimetric analysis, volume measurement and correlation of mass and volume, showed acceptable uniformity of 3D screen-/stencil-printed microtablets. In vivo experiments confirmed the rationale behind the concept. Conventional LG/permeation enhancer tablets of standard shape and size (T1), which begin to dissolve after intake, can only increase the bioavailability of LG by a factor of 1.8 compared with the LG tablet without a permeation enhancer. However, the bioavailability can be significantly increased by releasing LG faster and more precisely in the small intestine. Microtablets protected by an enteric capsule from dissolution in the stomach achieved higher bioavailability. The formulation containing both permeation enhancers, C8 and C10, achieved a 4.0-fold increase in relative bioavailability; with C10 alone, the increase was as high as 4.6-fold. Next, we investigated whether this approach could also be applied to another GLP inhibitor, SG. SG was formulated together with the permeation enhancer C10 and Labrasol as a solubilizer into microtablets, which were then packed into enteric capsules. Their bioavailability was measured against commercially available Rybelsus®. It is based on the permeation enhancer SNAC, which enables peptide absorption as early as in the stomach. In the animal studies conducted here, our new dosage form demonstrated higher systemic drug exposure compared to Rybelsus®. The numerical relative bioavailability of the new candidate, T5, is 940%, compared to Rybelsus®. Benchmarking against Rybelsus® provides insights into the absolute oral bioavailability of T5. Rybelsus® is reported to have an absolute oral bioavailability of approximately 0.4–1.0% [35], providing an initial angle towards this metric for T5. Although this comparison is indirect and must therefore be treated with caution, it highlights the potential of the proposed formulation concept to improve the oral delivery of peptide therapeutics.

While the present work is an encouraging initial proof of concept, the limitations of the study should be considered. In vivo experiments were conducted as pilot studies, with only a limited number of animals in each group. Additionally, there was relatively high inter-animal variability. Furthermore, the design of the present study did not permit the individual contributions of the different formulation components to the observed systemic exposure to be distinguished. This is especially true of Labrasol®'s solubilizing contribution. The improved bioavailability is likely the result of several synergistic mechanisms. These include the enteric capsule and microtablet formulation protecting the peptide from gastric degradation, enhanced intestinal permeation mediated by incorporated permeation enhancers, potential stabilization of the peptide through interactions with lipid-based excipients or micellar structures, and site-specific release in the distal small intestine. Understanding the relative contribution of each of these mechanisms still needs to be determined and requires additional experiments. A systematic analysis of the relevant formulations requires numerous comparison groups and, consequently, a large number of animals. Due to the high variability in the AUC among the animals, it might be more effective to select the best candidates through in vitro testing. We are planning experiments using Caco-2 cell monolayers to systematically compare various formulation approaches in vitro before testing the most promising ones in vivo. Additionally, comparing the pastes systematically to the material from the dissolved tablets will enable us to determine whether the printing process compromises the functional integrity of the APIs.

5. Conclusions

This study was designed to test concepts enabled by SPID® technology that could improve the bioavailability of oral peptide dosage forms. This is the first time that the possibility of using SPID® technology to manufacture oral peptide dosage forms with meaningful bioavailability has been established. The flexibility of SPID® technology made it possible to test several concepts, some of which yielded promising results. Further studies are intended to systematically develop the pilot candidates.

6. Patents

The use of 3DSP technology for the production of microtablets with LG or SG described here is legally protected by numerous patents (WO2025247506A1, WO2025247509A1, US12290607B2, US2023/0078273 A1, WO2019/129360 A1, US2016121599, WO2020127388, etc.).

Author Contributions: Conceptualization, E.A., P.N., M.E., A.S. (Achim Schneeberger) and K.K.; methodology, E.A., M.E., P.N. and P.H.; software, P.N.; validation, M.E., M.B. and E.A.; formal analysis, M.E.; investigation, E.A., M.E., P.N., P.H., H.L. and A.S. (Anne Seidlitz); resources, K.K.; data curation, P.N., P.H. and H.L.; writing—original draft preparation, P.N., E.A., M.E., M.B., P.H., H.L., A.B.-L., A.S. (Anne Seidlitz) and A.S. (Achim Schneeberger); writing—review and editing, P.N., E.A., M.E., M.B., P.H., A.B.-L., A.S. (Anne Seidlitz) and A.S. (Achim Schneeberger); visualization, P.N., M.E., A.S. (Anne Seidlitz), P.H. and H.L.; supervision, A.S. (Achim Schneeberger); project administration, E.A., M.E., P.N. and A.S. (Achim Schneeberger); funding acquisition, A.S. (Achim Schneeberger) and K.K. All authors have read and agreed to the published version of the manuscript.

Funding: This project was funded partly by the Ministry of Economy, Science and Digital Society, Free State of Thuringia (program: Thüringen Motivation; 2024 INP 0153). Financial support from the Thüringer Aufbaubank (TAB; WE 258174) is gratefully acknowledged.

Institutional Review Board Statement: Permission for the pig study was granted by the Austrian Animal Welfare Council (GZ: 2024-0.885.780, approved on 20 December 2024).

Informed Consent Statement: Not applicable.

Data Availability Statement: The data presented in this study are available on request from the corresponding author.

Acknowledgments: The authors would like to thank Susanne Franzmann and Sabine Morgenstern for their excellent analytical and laboratory support, as well as Lisa Jescheck, Lisa Frunzke and Michelle Fischer for providing their printing expertise. Our special thanks go to Nicolle Schwarz, who contributed to the success of the project through critical discussion of the study design. The authors also thank Evonik Operations GmbH for providing Eudracap® Enteric capsules and Gattefossé for providing Labrasol® ALF free of charge. Furthermore, we thank Stefan Seyferth (TU Erlangen) for his analytical support with the dissolution measurement for T5. During the preparation of this manuscript, the authors used ChatGPT (GPT-5.5 Sol and GPT5.6 Sol) for limited language editing.

Conflicts of Interest: E.A., P.N. and M.E. are employees of Laxxon Medical GmbH. A.S. and K.K. are managing directors of Laxxon Medical GmbH and Laxxon Medical Corp. The remaining authors declare no conflicts of interest.

Abbreviations

The following abbreviations are used in this manuscript:

3DSP	Three-dimensional screen printing
ACN	Acetonitril
API	Active pharmaceutical ingredient
AUC_{inf}	Area Under the Concentration–Time Curve from time zero extrapolated to infinity

AUC_{last}	Area Under the Concentration–Time Curve from time zero to the last measurable concentration
bw	Body weight
C10	Sodium caprate/sodium decanoate
C8	Sodium caprylate/sodium octanoate
CD	Circular dichroism
GLP-1	Glucagon-Like Peptide-1
GLP-1-RA	Glucagon-Like Peptide-1 Receptor Agonist
HPC	Hydroxypropyl cellulose
HPLC	High-Performance Liquid Chromatography
HPLC-MS/MS	High-Performance Liquid Chromatography coupled with Tandem Mass Spectrometry
HPMC	Hydroxypropylmethyl cellulose
LC-HRMS	Liquid Chromatography–High-Resolution Mass Spectrometry
LG	Liraglutide
RT	Room temperature
RSD	Relative Standard Deviation
SA/V	Surface area-to-volume ratio
s.c.	Subcutaneous
SD	Standard deviation
SG	Semaglutide
SNAC	N-(8-[2-hydroxybenzoyl]amino) caprylate
SPID®	Screen Printed Innovative Drugs
Tab, T	Tablet
USP	United States Pharmacopeia

Appendix A

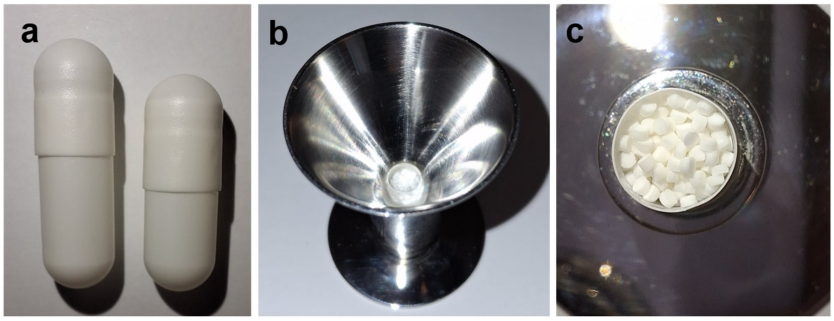

Figure A1. Precapped and closed Eudracap® Enteric capsule (Size 0) (**a**), ProFunnel Kit (#000-5), Profill (TORPAC, Fairfield, USA) for filling the capsules (**b**) and the capsule filled with microtablets in detail (**c**).

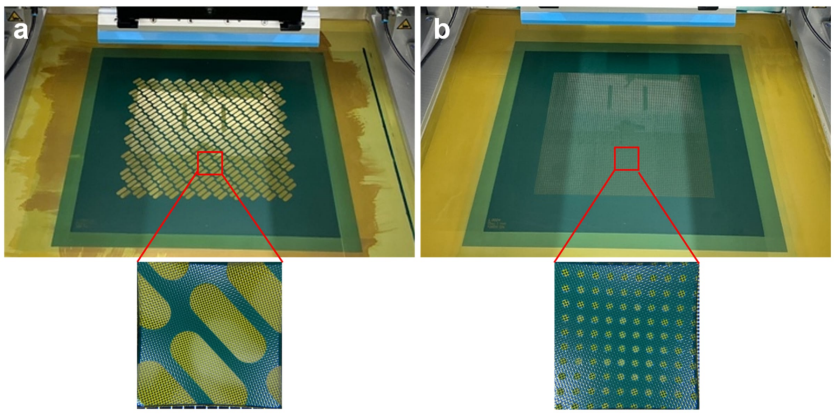

Figure A2. Screen layouts for printing the oval tablet T1 with 14 × 5 mm, yielding 389 tablets (**a**), and the T2 microtablets with a diameter of 1 mm, yielding 10,609 tablets (**b**).

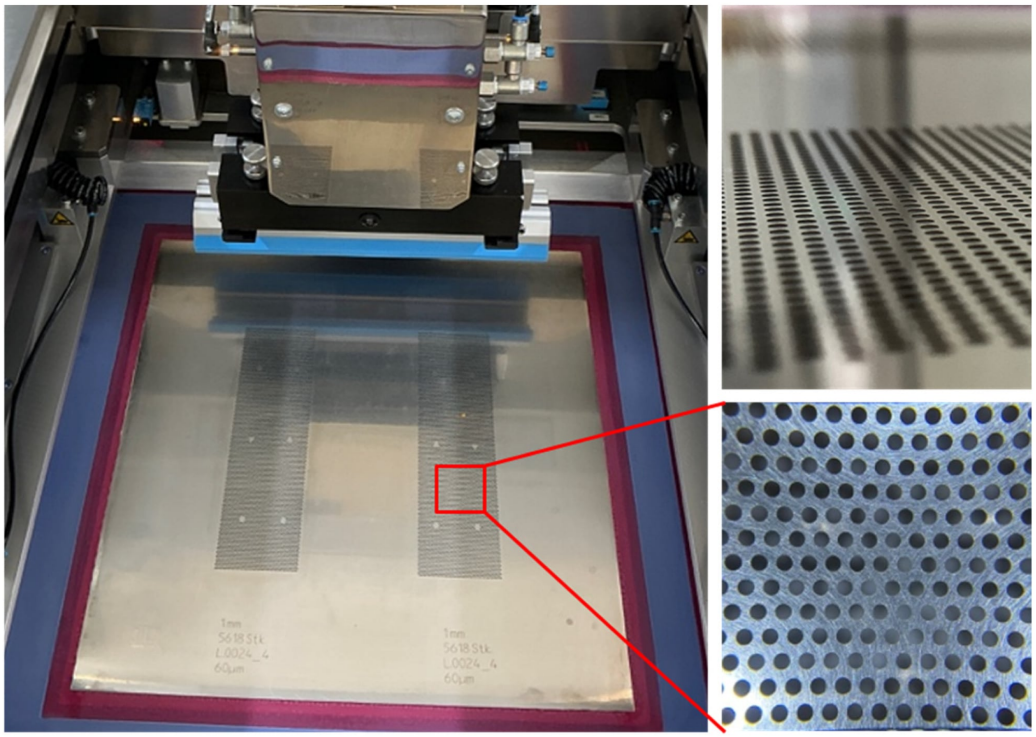

Figure A3. Stainless-steel stencil with a thickness of 60 µm for printing 5618 T3, T4 and T5 microtablets with a diameter of 1 mm.

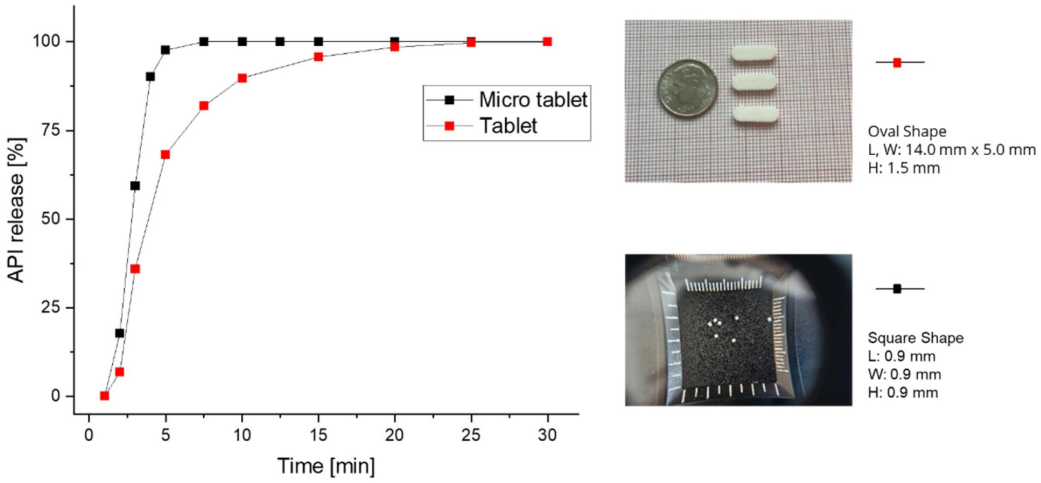

Figure A4. Comparison of the geometry and in vitro dissolution profiles of a conventionally compressed tablet and 3D screen-printed microtablets.

The conventional oval-shaped tablet (14 × 5 × 1.5 mm) exhibited a surface area-to-volume ratio (SA/V) of 1.85, whereas the square-shaped microtablets (0.9 × 0.9 × 0.9 mm) exhibited a substantially higher SA/V of 6.67. Acetaminophen was used as a model drug to evaluate the hypothesis that the increased surface area-to-volume ratio of the microtablets would accelerate drug dissolution and release compared with a conventional tablet. As expected, the microtablets achieved almost complete drug release within approximately 5–7 min, whereas the conventional tablet required approximately 20 min.

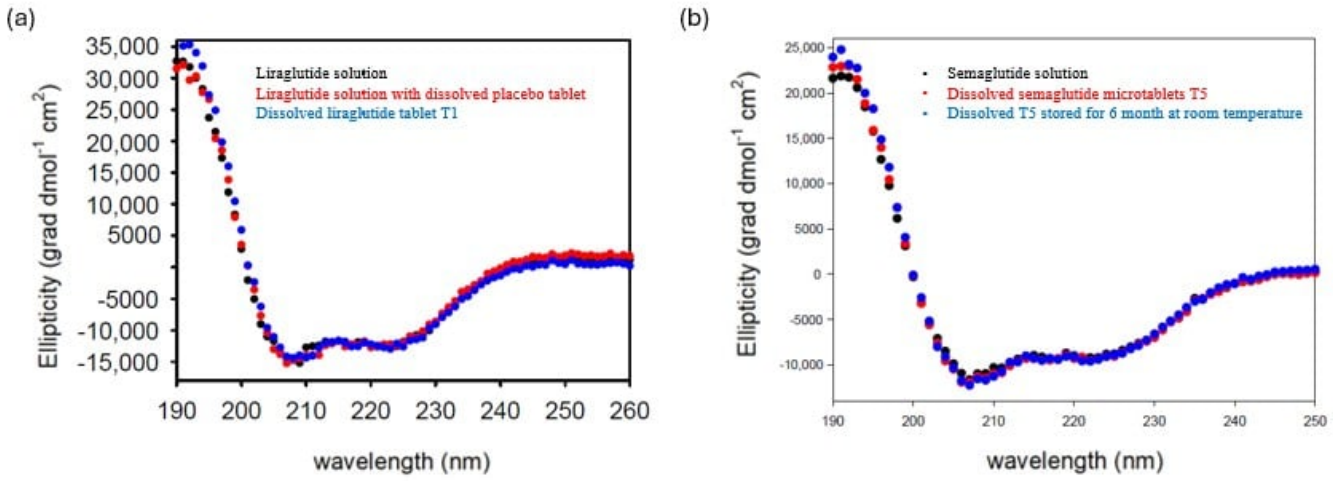

Figure A5. Circular dichroism (CD) of liraglutide (LG) and semaglutide (SG). (**a**) Far-UV CD spectra of LG in aqueous solution (black), in the presence of a dissolved placebo tablet (red), and released from the dissolved T1 tablet (blue). (**b**) Far-UV circular dichroism (CD) spectra of SG in aqueous solution (black); SG released from freshly produced dissolved T5 microtablets (red); and SG released from the dissolved T5 tablet, which was stored for 6 months at room temperature (blue). CD measurements were performed at 20 °C using a Jasco J-810 spectropolarimeter. The largely overlapping CD spectra indicate comparable secondary structural characteristics of LG and SG in the reference solutions and the printed tablet formulation.

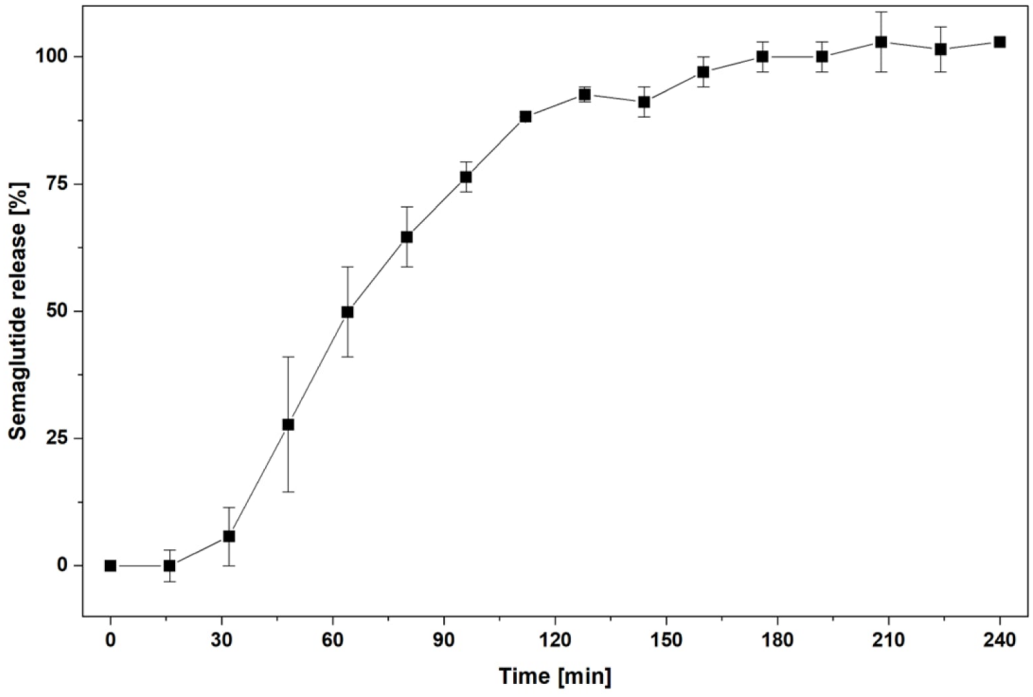

Figure A6. Release profiles of the semaglutide-containing T5 microtablets filled into enteric capsules in neutral medium (pH 6.85) for 4 h. The data are presented as MW ± SD, $n = 2$.

Table A1. Masses of the microtablet batches T2-T5 weighed into individual capsules to achieve a target fill mass of approximately 15 mg liraglutide/semaglutide per capsule.

Microtablet no.	Capsule no.	m (Microtablets) [mg]	API
T2	K1	300.63	Liraglutide
	K2	300.17	Liraglutide
	K3	300.52	Liraglutide
	K4	300.10	Liraglutide
T3	K1	300.57	Liraglutide
	K2	300.39	Liraglutide
	K3	300.51	Liraglutide
	K4	300.41	Liraglutide
T4	K1	300.08	Liraglutide
	K2	300.09	Liraglutide
	K3	300.12	Liraglutide
	K4	300.02	Liraglutide
T5	K1	300.28	Semaglutide
	K2	300.17	Semaglutide
	K3	300.34	Semaglutide

Table A2. HPLC gradient elution conditions.

Time [min]	Flowrate [mL/min]	Solution A [v/v%]	Solution B [v/v%]
0.00	0.20	68	32
0.70	0.20	68	32
6.30	0.20	45	55
16.10	0.20	45	55
20.00	0.20	68	32
26.00	0.20	68	32

Table A3. Mass spectrometric acquisition parameters used for the quantification of liraglutide and in pig plasma by LC-HRMS.

Parameter	Setting
Mass spectrometer	Q Exactive Orbitrap
Ionization source	Heated electrospray ionization (H-ESI2)
Ionization mode	Positive (ESI+)
Acquisition mode	Parallel reaction monitoring (PRM)
Collision energy	15
Liraglutide quantitation ion (m/z)	1128.65
Internal standard	d-liraglutide
d-liraglutide quantitation ion (m/z)	946.543
Spray voltage	4 kV
Sheath gas	45

Table A3. *Cont.*

Parameter	Setting
Auxiliary gas	20
Spare gas	2
Capillary temperature	350 °C
H-ESI2 heater temperature	350 °C
Mass resolution	35,000
Mass tolerance	20 mmu

Table A4. Mass spectrometric acquisition parameters used for the quantification of semaglutide in pig plasma.

Parameter	Setting
Mass spectrometer	Q Exactive Orbitrap
Ionization source	Heated electrospray ionization (H-ESI2)
Ionization mode	Positive (ESI+)
Acquisition mode	Parallel reaction monitoring (PRM)
Collision energy	10
Semaglutide quantitation ion (m/z)	1028.7866
Internal standard	Diclofenac
d-quantitation ion (m/z)	296.024
Spray voltage	4 kV
Sheath gas	45
Auxiliary gas	20
Spare gas	2
Capillary temperature	350 °C
H-ESI2 heater temperature	350 °C
Mass resolution	70,000
Mass tolerance	10 mmu

Table A5. Galenic parameters for tablet T1.

Parameter	Value
Hardness [a]	40.5 ± 0.2 N
Friability [b]	0.12%
Mass uniformity [c]	85.6 ± 4.3 mg
Dimension uniformity [c]	13.29 ± 0.39 mm × 4.55 ± 0.36 mm × 1.94 ± 0.07 mm

(a) The fracture resistance of tablets was detected using a tablet hardness testing instrument, the PTB 51 1E manufactured by Pharma Test (Apparatebau AG; Hainburg, Germany), according to Ph. Eur. 2.9.8. The average and standard deviation of 10 randomly selected tablets was calculated. (b) Friability was tested as described in Ph. Eur. 2.9.7. Deviating from the method, 10 tablets were dedusted by airflow and weighed, then rotated 100 times at 25 rpm on a single-drum tablet friability test instrument, the PTF 100 manufactured by Pharma Test (Apparatebau AG; Hainburg, Germany). Friability was determined as the percentage of weight loss after a further dedusting of the tablets. (c) Mass uniformity and dimension uniformity were measured from 10 random tablets with the help of a semi-automated tablet tester, the P5, manufactured by Kraemer Elektronik GmbH, Darmstadt, Germany.

References

1. Drucker, D.J. Mechanisms of action and therapeutic application of glucagon-like peptide-1. *Cell Metab.* **2018**, *27*, 740–756. [CrossRef] [PubMed]
2. Thota-Kammili, S.; Tama, E.; Hurtado Andrade, M.D. Glucagon-like peptide 1 receptor agonists for obesity: Efficacy, side effects, and risks. *Curr. Treat. Options Gastroenterol.* **2024**, *22*, 145–154. [CrossRef]
3. Li, J.; Zheng, J.; Wang, S.; Lau, H.K.; Fathi, A.; Wang, Q. Cardiovascular benefits of native GLP-1 and its metabolites: An indicator for GLP-1-therapy strategies. *Front. Physiol.* **2017**, *8*, 15. [CrossRef] [PubMed]
4. Moiz, A.; Filion, K.B.; Tsoukas, M.A.; Yu, O.H.; Peters, T.M.; Eisenberg, M.J. The expanding role of GLP-1 receptor agonists: A narrative review of current evidence and future directions. *eClinicalMedicine* **2025**, *86*, 103363. [CrossRef] [PubMed]
5. Chen, J.; Mei, A.; Wei, Y.; Li, C.; Qian, H.; Min, X.; Yang, H.; Dong, L.; Rao, X.; Zhong, J. GLP-1 receptor agonist as a modulator of innate immunity. *Front. Immunol.* **2022**, *13*, 997578. [CrossRef] [PubMed]
6. Zhao, X.; Wang, M.; Wen, Z.; Lu, Z.; Cui, L.; Fu, C.; Xue, H.; Liu, Y.; Zhang, Y. GLP-1 receptor agonists: Beyond their pancreatic effects. *Front. Endocrinol.* **2021**, *12*, 721135. [CrossRef] [PubMed]
7. Al Qassab, M.; Mneimneh, M.; Jradi, A.; Derbas, B.; Dabboussi, D.; Baini, J.K.; Katrib, N.; Chaarani, N.; Attieh, P.; Kanaan, A.; et al. The expanding role of GLP-1 receptor agonists: Advancing clinical outcomes in metabolic and mental health. *Curr. Issues Mol. Biol.* **2025**, *47*, 285. [CrossRef] [PubMed]
8. Mentlein, R. Mechanisms underlying the rapid degradation and elimination of the incretin hormones GLP-1 and GIP. *Best Pract. Res. Clin. Endocrinol. Metab.* **2009**, *23*, 443–452. [CrossRef] [PubMed]
9. Klemann, C.; Wagner, L.; Stephan, M.; von Hörsten, S. Cut to the chase: A review of CD26/dipeptidyl peptidase-4's (DPP4) entanglement in the immune system. *Clin. Exp. Immunol.* **2016**, *185*, 1–21. [CrossRef] [PubMed]
10. Zhong, J.; Gong, Q.; Goud, A.; Srinivasamaharaj, S.; Rajagopalan, S. Recent advances in dipeptidyl-peptidase-4 inhibition therapy: Lessons from the bench and clinical trials. *J. Diabetes Res.* **2015**, *2015*, 606031. [CrossRef] [PubMed]
11. Lee, S.; Lee, D.Y. Glucagon-like peptide-1 and glucagon-like peptide-1 receptor agonists in the treatment of type 2 diabetes. *Ann. Pediatr. Endocrinol. Metab.* **2017**, *22*, 15–26. [CrossRef] [PubMed]
12. Jacobsen, L.V.; Flint, A.; Olsen, A.K.; Ingwersen, S.H. Liraglutide in type 2 diabetes mellitus: Clinical pharmacokinetics and pharmacodynamics. *Clin. Pharmacokinet.* **2016**, *55*, 657–672. [CrossRef] [PubMed]
13. Dhillon, S. Semaglutide: First global approval. *Drugs* **2018**, *78*, 275–284. [CrossRef] [PubMed]
14. Marbury, T.C.; Flint, A.; Jacobsen, J.B.; Karsbøl, J.D.; Lasseter, K. Pharmacokinetics and tolerability of a single dose of semaglutide, a human glucagon-like peptide-1 analog, in subjects with and without renal impairment. *Clin. Pharmacokinet.* **2017**, *56*, 1381–1390. [CrossRef] [PubMed]
15. American Diabetes Association Professional Practice Committee. 9. Pharmacologic approaches to glycemic treatment: Standards of care in diabetes—2024. *Diabetes Care* **2023**, *47*, S158. [CrossRef] [PubMed]
16. Boye, K.; Ross, M.; Mody, R.; Konig, M.; Gelhorn, H. Patients' preferences for once-daily oral versus once-weekly injectable diabetes medications: The REVISE study. *Diabetes Obes. Metab.* **2021**, *23*, 508–519. [CrossRef] [PubMed]
17. Garvey, W.T.; Batterham, R.L.; Bhatta, M.; Buscemi, S.; Christensen, L.N.; Frias, J.P.; Jódar, E.; Kandler, K.; Rigas, G.; Wadden, T.A.; et al. Two-year effects of semaglutide in adults with overweight or obesity: The STEP 5 trial. *Nat. Med.* **2022**, *28*, 2083–2091. [CrossRef] [PubMed]
18. Granhall, C.; Donsmark, M.; Blicher, T.M.; Golor, G.; Søndergaard, F.L.; Thomsen, M.; Bækdal, T.A. Safety and Pharmacokinetics of Single and Multiple Ascending Doses of the Novel Oral Human GLP-1 Analogue, Oral Semaglutide, in Healthy Subjects and Subjects with Type 2 Diabetes. *Clin. Pharmacokinet.* **2019**, *58*, 781–791. [CrossRef] [PubMed]
19. Wharton, S.; Lingvay, I.; Bogdanski, P.; Vale, R.D.D.; Jacob, S.; Karlsson, T.; Shaji, C.; Rubino, D.; Garvey, W.T. Oral semaglutide at a dose of 25 mg in adults with overweight or obesity. *N. Engl. J. Med.* **2025**, *393*, 1077–1087. [CrossRef] [PubMed]
20. Ojinna, B.T.; Tariq, S.; Agho, O.; Channa, R.; Singh, G. A Review of the Oral Semaglutide in Adults with Overweight or Obesity (OASIS) Trials Evaluating Oral Semaglutide (Wegovy) for Chronic Weight Management in Adults with Overweight or Obesity. *Cureus* **2026**, *18*, e107970. [CrossRef] [PubMed]
21. Tuvia, S.; Pelled, D.; Marom, K.; Salama, P.; Levin-Arama, M.; Karmeli, I.; Idelson, G.H.; Landau, I.; Mamluk, R. A Novel Suspension Formulation Enhances Intestinal Absorption of Macromolecules Via Transient and Reversible Transport Mechanisms. *Pharm. Res.* **2014**, *31*, 2010–2021. [CrossRef] [PubMed]
22. Johns, D.G.; Campeau, L.-C.; Banka, P.; Bautmans, A.; Bueters, T.; Bianchi, E.; Branca, D.; Bulger, P.G.; Crevecoeur, I.; Ding, F.-X.; et al. Orally Bioavailable Macrocyclic Peptide That Inhibits Binding of PCSK9 to the Low Density Lipoprotein Receptor. *Circulation* **2023**, *148*, 144–158. [CrossRef] [PubMed]
23. Ballantyne, C.M.; Gellis, L.; Tardif, J.C.; Banka, P.; Navar, A.M.; Asprusten, E.A.; Scott, R.; Stroes, E.S.G.; Froman, S.; Mendizabal, G.; et al. Efficacy and Safety of Oral PCSK9 Inhibitor Enlicitide in Adults With Heterozygous Familial Hypercholesterolemia: A Randomized Clinical Trial. *JAMA* **2026**, *335*, 129–139. [PubMed]

24. Overgaard, R.V.; Navarria, A.; Ingwersen, S.H.; Bækdal, T.A.; Kildemoes, R.J. Clinical pharmacokinetics of oral semaglutide: Analyses of data from clinical pharmacology trials. *Clin. Pharmacokinet.* **2021**, *60*, 1335–1348. [CrossRef] [PubMed]
25. Buckley, S.T.; Bækdal, T.A.; Vegge, A.; Maarbjerg, S.J.; Pyke, C.; Ahnfelt-Rønne, J.; Madsen, K.G.; Schéele, S.G.; Alanentalo, T.; Kirk, R.K.; et al. Transcellular stomach absorption of a derivatized glucagon-like peptide-1 receptor agonist. *Sci. Transl. Med.* **2018**, *10*, eaar7047. [CrossRef] [PubMed]
26. Novo Nordisk Inc. *RYBELSUS® (Semaglutide) Tablets, for Oral Use: Prescribing Information*; Novo Nordisk Inc.: Plainsboro, NJ, USA, 2024.
27. Brayden, D.J.; Maher, S. Transient Permeation Enhancer® (TPE®) technology for oral delivery of octreotide: A technological evaluation. *Expert Opin. Drug Deliv.* **2021**, *18*, 1501–1512. [CrossRef] [PubMed]
28. Leonard, T.W.; Lynch, J.; McKenna, M.J.; Brayden, D.J. Promoting absorption of drugs in humans using medium-chain fatty acid-based solid dosage forms: GIPET™. *Expert Opin. Drug Deliv.* **2006**, *3*, 685–692. [CrossRef] [PubMed]
29. Maher, S.; Brayden, D.J.; Casettari, L.; Illum, L. Application of permeation enhancers in oral delivery of macromolecules: An update. *Pharmaceutics* **2019**, *11*, 41. [CrossRef] [PubMed]
30. Kim, J.C.; Park, E.J.; Na, D.H. Gastrointestinal permeation enhancers for the development of oral peptide pharmaceuticals. *Pharmaceuticals* **2022**, *15*, 1585. [CrossRef] [PubMed]
31. Walsh, E.G.; Adamczyk, B.E.; Chalasani, K.B.; Maher, S.; O'Toole, E.B.; Fox, J.S.; Leonard, T.W.; Brayden, D.J. Oral delivery of macromolecules: Rationale underpinning Gastrointestinal Permeation Enhancement Technology (GIPET®). *Ther. Deliv.* **2011**, *2*, 1595–1610. [CrossRef] [PubMed]
32. Krug, S.M.; Amasheh, M.; Dittmann, I.; Christoffel, I.; Fromm, M.; Amasheh, S. Sodium caprate as an enhancer of macromolecule permeation across tricellular tight junctions of intestinal cells. *Biomaterials* **2013**, *34*, 275–282. [CrossRef] [PubMed]
33. Raoof, A.A.; Chiu, P.; Ramtoola, Z.; Cumming, I.K.; Teng, C.; Weinbach, S.P.; Hardee, G.E.; Levin, A.A.; Geary, R. Oral bioavailability and multiple dose tolerability of an antisense oligonucleotide tablet formulated with sodium caprate. *J. Pharm. Sci.* **2004**, *93*, 1431–1439. [CrossRef] [PubMed]
34. Twarog, C.; Fattah, S.; Heade, J.; Maher, S.; Fattal, E.; Brayden, D.J. Intestinal permeation enhancers for oral delivery of macromolecules: A comparison between salcaprozate. sodium (SNAC) and sodium caprate (C_{10}). *Pharmaceutics* **2019**, *11*, 78. [CrossRef] [PubMed]
35. U.S. Food and Drug Administration. RYBELSUS® (semaglutide) tablets, for oral use. In *Prescribing Information*; U.S. Food and Drug Administration: Silver Spring, MD, USA, 2024.
36. Fagan, A.; Bateman, L.; O'MAhony, M.; Crean, A.; O'SHea, J. Direct compression peptide tablets: Insights into the importance of permeation enhancer processibility and peptide stability. *Int. J. Pharm.* **2025**, *685*, 126257. [CrossRef] [PubMed]
37. Xu, P.; Nguyen, H.T.; Huang, S.; Tran, H. Development of 3D-Printed Two-Compartment Capsular Devices for Pulsatile Release of Peptide and Permeation Enhancer. *Pharm. Res.* **2024**, *41*, 2259–2270. [CrossRef] [PubMed]
38. Blümlinger, M.; Hamar, F.; Werle, M.; Föger, F.; Hrouda, M.; Ludewig, E.; Huck, C.; Heiss, M.; Schwarz, L. Ileum targeted semaglutide delivery and pharmacokinetic study in an experimental porcine animal model via oesophagogastroduodenoscopic administration. *J. Control. Release* **2025**, *387*, 114164. [CrossRef] [PubMed]
39. Moldenhauer, D.; Nguyen, D.C.Y.; Jescheck, L.; Hack, F.; Fischer, D.; Schneeberger, A. 3D screen printing–An innovative technology for large-scale manufacturing of pharmaceutical dosage forms. *Int. J. Pharm.* **2021**, *592*, 120096. [CrossRef] [PubMed]
40. Markl, D.; Zeitler, J.A. A Review of Disintegration Mechanisms and Measurement Techniques: Markl and Zeitler. *Pharm. Res.* **2017**, *34*, 890–917. [CrossRef] [PubMed]
41. Noyes, A.A.; Whitney, W.R. The rate of solution of solid substances in their own solutions. *J. Am. Chem. Soc.* **1897**, *19*, 930–934. [CrossRef]
42. Nernst, W. Theorie der Reaktionsgeschwindigkeit in heterogenen Systemen. *Z. Für Phys. Chem.* **1904**, *47*, 52–55. [CrossRef]
43. Brunner, E. *Reaktionsgeschwindigkeit in Heterogenen Systemen*; Georg-Augusts-Universitat: Gottingen, Germany, 1903.
44. Brayden, D.J. Localised Delivery of Macromolecules to the Large Intestine: Translation to Clinical Trials: DJ Brayden. *BioDrugs* **2022**, *36*, 687–700. [CrossRef] [PubMed]
45. Brayden, D.J. Per Artursson's major contributions to the Caco-2 cell literature in pharmaceutical sciences. *J. Pharm. Sci.* **2021**, *110*, 12–16. [CrossRef] [PubMed]
46. Twarog, C.; Fattal, E.; Noiray, M.; Illel, B.; Brayden, D.J.; Taverna, M.; Hillaireau, H. Characterization of the physicochemical interactions between exenatide and two intestinal permeation enhancers: Sodium caprate (C_{10}) and salcaprozate sodium (SNAC). *Int. J. Pharm.* **2022**, *626*, 122131. [CrossRef] [PubMed]
47. Koga, K.; Kusawake, Y.; Ito, Y.; Sugioka, N.; Shibata, N.; Takada, K. Enhancing mechanism of Labrasol on intestinal membrane permeability of the hydrophilic drug gentamicin sulfate. *Eur. J. Pharm. Biopharm.* **2006**, *64*, 82–91. [CrossRef] [PubMed]
48. Dalsaniya, G.; Bhalani, D.; Jasoliya, D.; Shukla, A.; Ray, D.; Aswal, V.K.; Pillai, S.A. Labrasol® Micelles as Next-Generation Nanomedicine: Characterization, Encapsulation, and Cytotoxicity of Quercetin and Curcumin for Lung Cancer Treatment. *ChemistrySelect* **2025**, *10*, e03320. [CrossRef]

49. Kaur, J.; Singla, P.; Kaur, I. Labrasol mediated enhanced solubilization of natural hydrophobic drugs in Pluronic micelles: Physicochemical and in vitro release studies. *J. Mol. Liq.* **2022**, *361*, 119596. [CrossRef]
50. Aguirre, T.; Teijeiro-Osorio, D.; Rosa, M.; Coulter, I.; Alonso, M.; Brayden, D. Current status of selected oral peptide technologies in advanced preclinical development and in clinical trials. *Adv. Drug Deliv. Rev.* **2016**, *106*, 223–241. [CrossRef] [PubMed]
51. Brayden, D.; Hill, T.; Fairlie, D.; Maher, S.; Mrsny, R. Systemic delivery of peptides by the oral route: Formulation and medicinal chemistry approaches. *Adv. Drug Deliv. Rev.* **2020**, *157*, 2–36. [CrossRef] [PubMed]
52. Enke, M.; Bünger, M.; Aedtner, E.; Kastner, S.; Gruschwitz, F.; Kühne, K.; Czernik-Schulz, D.; Greeley, D.R.; Volc, D.; Buzachnich-Ladinig, A.; et al. Three-Dimensional Screen Printing Technology Enables Sequential Release of Carbidopa and Levodopa—A New Approach Improving Levodopa Delivery for Treating Parkinson's Disease. *Pharmaceutics* **2025**, *17*, 1507. [CrossRef] [PubMed]
53. Enke, M.; Schwarz, N.; Gruschwitz, F.; Winkler, D.; Hanf, F.; Jescheck, L.; Seyferth, S.; Fischer, D.; Schneeberger, A. 3D screen printing technology enables fabrication of oral drug dosage forms with freely tailorable release profiles. *Int. J. Pharm.* **2023**, *642*, 123101. [CrossRef] [PubMed]
54. Schneeberger, A.; Enke, M.; Kühne, K.; Seyferth, S.; Fischer, D. 3D screen printing enables application of integrated QR codes on pharmaceutical dosage forms in mass production—A game changer. *Biomed. J. Sci. Tech. Res.* **2022**, *41*, 32889–32895. [CrossRef]
55. Schwarz, N.; Enke, M.; Gruschwitz, F.V.; Winkler, D.; Franzmann, S.; Jescheck, L.; Hanf, F.; Schneeberger, A. 3D Screen Printing Offers Unprecedented Anticounterfeiting Strategies for Oral Solid Dosage Forms Feasible for Large Scale Production. *Pharmaceutics* **2024**, *16*, 368. [CrossRef] [PubMed]
56. Schneeberger, A.; Seyferth, S.; Fischer, D. Scalable 3D Screen Printing Technology in Pharmaceutical Manufacturing-High Degree of Freedom in Terms of Drug Choice. *Arch. Dent.* **2021**, *3*, 19–21. [CrossRef]

Disclaimer/Publisher's Note: The statements, opinions and data contained in all publications are solely those of the individual author(s) and contributor(s) and not of MDPI and/or the editor(s). MDPI and/or the editor(s) disclaim responsibility for any injury to people or property resulting from any ideas, methods, instructions or products referred to in the content.